VEGF-C/VEGFR-3 signalling in macrophages ameliorates acute lung injury

Masahiro Yamashita[1], Miyuki Niisato[1], Yasushi Kawasaki[2], Sinem Karaman[3], Marius R. Robciuc[3], Yuji Shibata[4], Yoji Ishida[5], Ryosuke Nishio[6], Tomoyuki Masuda[4], Tamotsu Sugai[4], Masao Ono[7], Rubin M. Tuder[8], Kari Alitalo[3] and Kohei Yamauchi[1]

[1]Dept of Pulmonary Medicine, Allergy and Immunological Diseases, Iwate Medical University School of Medicine, Morioka, Japan. [2]Dept of Health Chemistry, Iwate Medical University School of Pharmacology, Shiwa, Japan. [3]Wihuri Research Institute and Translational Cancer Medicine Program, University of Helsinki, Helsinki, Finland. [4]Dept of Pathology, Iwate Medical University School of Medicine, Shiwa, Japan. [5]Dept of Hematology, Iwate Medical University School of Medicine, Shiwa, Japan. [6]Nishio Cardiovascular Clinic, Kyoto, Japan. [7]Dept of Pathology, Tohoku University Graduate School of Medicine, Sendai, Japan. [8]Program in Translational Lung Research, Division of Pulmonary Sciences and Critical Care Medicine, Dept of Medicine, University of Colorado School of Medicine, Aurora, CO, USA.

Corresponding author: Masahiro Yamashita (yamam@iwate-med.ac.jp)

Shareable abstract (@ERSpublications)
VEGF-C/VEGFR-3 signals on macrophages ameliorate acute lung injury *via* multiple functions, including increased anti-inflammatory cytokine production and increased efferocytosis, and VEGFR-3 expression on macrophages is impaired in human ARDS https://bit.ly/3D8Au3j

Cite this article as: Yamashita M, Niisato M, Kawasaki Y, *et al*. VEGF-C/VEGFR-3 signalling in macrophages ameliorates acute lung injury. *Eur Respir J* 2022; 59: 2100880 [DOI: 10.1183/13993003.00880-2021].

This article has an editorial commentary: https://doi.org/10.1183/13993003.03000-2021

Received: 16 Jan 2020
Accepted: 14 Aug 2021

Abstract

Background Successful recovery from acute lung injury requires inhibition of neutrophil influx and clearance of apoptotic neutrophils. However, the mechanisms underlying recovery remain unclear. We investigated the ameliorative effects of vascular endothelial growth factor (VEGF)-C/VEGF receptor 3 (VEGFR-3) signalling in macrophages in lipopolysaccharide (LPS)-induced lung injury.

Methods LPS was intranasally injected into wild-type and transgenic mice. Gain and loss of VEGF-C/VEGFR-3 signalling function experiments employed adenovirus-mediated intranasal delivery of VEGF-C (Ad-VEGF-C vector) and soluble VEGFR-3 (sVEGFR-3) or anti-VEGFR-3 blocking antibodies and mice with a deletion of VEGFR-3 in myeloid cells.

Results The early phase of lung injury was significantly alleviated by the overexpression of VEGF-C with increased levels of bronchoalveolar lavage (BAL) fluid interleukin-10 (IL-10), but worsened in the later phase by VEGFR-3 inhibition upon administration of Ad-sVEGFR-3 vector. Injection of anti-VEGFR-3 antibodies to mice in the resolution phase inhibited recovery from lung injury. The VEGFR-3-deleted mice had a shorter survival time than littermates and more severe lung injury in the resolution phase. Alveolar macrophages in the resolution phase digested most of the extrinsic apoptotic neutrophils and VEGF-C/VEGFR-3 signalling increased efferocytosis *via* upregulation of integrin α_v in the macrophages. We also found that incubation with BAL fluid from acute respiratory distress syndrome (ARDS) patients, but not from controls, decreased VEGFR-3 expression and the efficiency of IL-10 expression and efferocytosis in human monocyte-derived macrophages.

Conclusions VEGF-C/VEGFR-3 signalling in macrophages ameliorates experimental lung injury. This mechanism may also provide an explanation for ARDS resolution.

Introduction

Pro-inflammatory stimuli cause rapid accumulation of neutrophils and macrophages in the lungs during the early stage of acute lung injury, to eliminate causal stimuli or organisms [1, 2]. During later phases, neutrophil influx is inhibited by anti-inflammatory cytokines, such as interleukin-10 (IL-10) [3, 4], and the subsequent elimination of apoptotic neutrophils from inflammatory lesions by a process known as efferocytosis, which is essential for successful resolution of inflammation [5–7]. Dysfunction of these

sequential processes causes irreversible lung tissue damage, as observed in severe types of acute respiratory distress syndrome (ARDS) [8]. ARDS is characterised by diffuse alveolar damage, a pathological lung injury pattern and increased neutrophils in bronchoalveolar lavage (BAL) fluid [9]. In the clinical setting, even if patients survive respiratory failure in the acute phase, prolonged mechanical ventilation may be required in severe ARDS, which is associated with high mortality [10–12]. Currently, there are very limited therapeutic strategies for such refractory conditions.

Macrophages are sources of various cytokines and are key cells in the elimination of apoptotic neutrophils [13–16]. Several molecules have been shown to participate in phagocytosis by macrophages [17–23]. In particular, an increasing body of evidence implicates the expression of integrin α_v (CD51) on phagocytes in efferocytosis *via* heterodimerisation with β_3 (CD51/CD61) or β_5 [21–23].

Macrophages also produce vascular endothelial growth factor (VEGF)-C, and VEGF-C/VEGF receptor 2 (VEGFR-3) signalling regulates lymphangiogenesis [24–28]. Interestingly, previous studies have also reported VEGFR-3 expression in macrophages, but its functions in pathological conditions are poorly known [29–32]. Zhang *et al.* [31] reported that VEGFR-3 signalling in macrophages contributes to prolonged survival in a sepsis model induced by intraperitoneal injection of lipopolysaccharide (LPS), limiting inflammation in the acute phase of sepsis.

Here, we elucidated the restorative effects of VEGFR-3$^+$ macrophages in LPS-induced lung injury and investigated the pathogenic relevance in human ARDS in order to provide a better mechanistic understanding of the resolution of lung injury.

Materials and methods

For full details, see the supplementary material.

Animal models

LPS was delivered intranasally to wild-type C57BL/6J, C57BL/6J-Tg(Csf1r-EGFP-NGFR/FKBP1A/TNFRSF6)2Bck/J [33] and LysM-specific VEGFR-3 knockout mice, which were produced by crossing LysM-Cre and VEGFR-3-floxed mice. To study the effect of gain and loss of VEGF-C/VEGFR-3 signalling, mice with myeloid cell-specific VEGFR-3 deletion were intranasally administered VEGF-C (Ad-VEGF-C vector) and soluble VEGFR-3 (sVEGFR-3) using an adenovirus vector [34, 35] or anti-VEGFR-3 blocking antibody. All animal experiments were approved by the Committee for Animal Experiments of Iwate Medical University (Morioka, Japan).

Experiments using human samples

The *in vitro* experiments evaluating the expression and function of VEGFR-3 in human macrophages employed BAL samples from healthy volunteers and patients with ARDS and cryptogenic organising pneumonia (COP) (patient characteristics are shown in supplementary table S1). Organising pneumonia is another pathological type of lung injury with enhanced BAL lymphocyte rates and excellent prognosis [9, 36]. The use of human samples was approved by the Ethics Committee of Iwate Medical University (H29-18). Informed consent was obtained from volunteers, patients or their families.

Results

LPS-induced lung injury model and lymphatic vessel perimeter

We administered LPS at 1.9 mg·kg^{-1} body weight intranasally to C57BL/6J mice, and then harvested BAL fluid and lung tissue samples on days 1, 2, 3, 4, 5 and 7. We observed increased BAL neutrophil counts on day 2 or 3, followed by a rapid reduction after day 4. In contrast, BAL macrophage counts increased on day 4, when neutrophil and macrophage counts were nearly equal (figure 1a–d). An increase in lymphocyte counts in BAL fluid was observed on day 7 post-LPS induction. The rates of macrophage and neutrophil counts relative to total blood cells showed no statistical differences between BAL fluid and tissue samples (supplementary figure S1a and b); in all experiments, hereafter, it was validated that no differences were found in blood cell count fractions between BAL fluid and tissue samples, except for neutrophil fractions between BAL fluid and tissue samples on day 1 in mice receiving Ad-VEGF-C vector (supplementary figure S1c–g). We estimated the injury score of tissue samples and BAL protein concentration. Their peaks were observed on day 3 (figure 1e and f).

We estimated the mRNA levels of VEGF-C and VEGF-D by quantitative real-time reverse transcription PCR (qRT-PCR) of cell pellets obtained from BAL by centrifugation. Increased *Vegfc* mRNA was observed in BAL mononuclear cells on day 4 after LPS injection, whereas no *Vegfd* mRNA was detected (figure 1g).

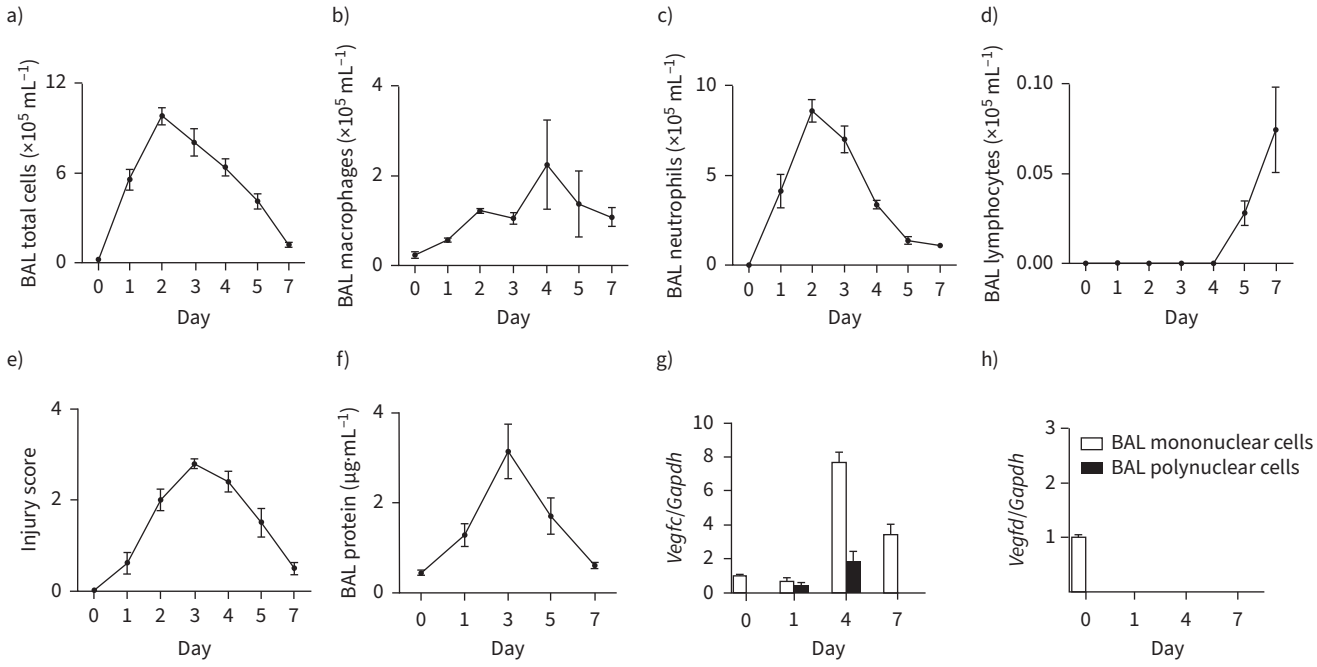

FIGURE 1 Kinetics of lipopolysaccharide (LPS)-induced lung injury. Mice (n=3 mice per treatment group) were intranasally injected with 1.9 mg·kg^{-1} body weight of LPS, and their bronchoalveolar lavage (BAL) fluid and lung tissue samples were harvested after 1, 2, 3, 4, 5 and 7 days. a–d) BAL total cell, macrophage, neutrophil and lymphocyte counts. e) Injury score. f) BAL protein concentration. g, h) Relative expression levels of g) *Vegfc* and g) *Vegfd* mRNA using *Gapdh* mRNA levels for normalisation in mononuclear and polynuclear cell pellets obtained from BAL were determined by real-time reverse transcription PCR. Data are presented as mean±SEM.

Effects of VEGF-C and sVEGFR-3-Ig during LPS-induced lung injury

Intranasal administration of Ad-LacZ, Ad-VEGF-C and Ad-sVEGFR-3-Ig vectors did not dramatically affect BAL cell counts (supplementary figure S2a). The levels of human VEGF-C, estimated *via* ELISA, were elevated between days 3 and 7 (supplementary figure S2b). Relative intensities of sVEGFR-3-Ig in BAL fluid estimated by immunoblotting were also higher between days 3 and 7 than at earlier and later time-points (supplementary figure S2c and d).

In the lung injury model using LPS, BAL total cell and neutrophil counts were decreased more significantly in mice that received Ad-VEGF-C vector than in mice that received Ad-LacZ vector on day 1 (figure 2a–c and supplementary figure S1c). In addition, injury scores and BAL protein concentration were significantly decreased in mice that received Ad-VEGF-C vector on days 1 and 4, respectively (figure 2d and e). In addition, BAL monocyte chemotactic protein-1 (MCP-1) and IL-10 protein levels were higher in mice that received Ad-VEGF-C vector than in those that received Ad-LacZ vector (figure 2f–g). BAL C-X-C motif chemokine ligand 1 (CXCL1), CXCL2, IL-1β, tumour necrosis factor-α (TNF-α), IL-6 and IL-17A protein did not differ between these two groups on day 1 and/or day 4 (supplementary figure S2f–k). These results indicate that VEGF-C/VEGFR-3 signals play an anti-inflammatory role, as indicated by the increased expression of IL-10.

In contrast, BAL neutrophil counts, injury score and protein concentrations on day 4 were higher in mice that received the Ad-sVEGFR-3-Ig vector than in mice with the Ad-LacZ vector, but no differences were observed on day 1 (figure 2h–n, and supplementary figures S1d–e and S2l–q). BAL MCP-1 levels decreased significantly on day 1 in mice that received Ad-sVEGFR-3-Ig vector compared with mice that received Ad-LacZ vector, although the concentrations of BAL IL-10, CXCL1, CXCL2, IL-1β, TNF-α and IL-6 proteins were not altered (figure 2n and o, and supplementary figure S2l–o).

To determine whether VEGF-C/VEGFR-3 signals are uniquely involved in the recovery phase of the lung injury model other than anti-inflammatory effects in the early phase, anti-VEGFR-3 blocking antibodies were administered starting on day 3, when lung injury had fully developed, and then harvested on day 5. Neutrophil counts and injury scores were increased more significantly in mice treated with

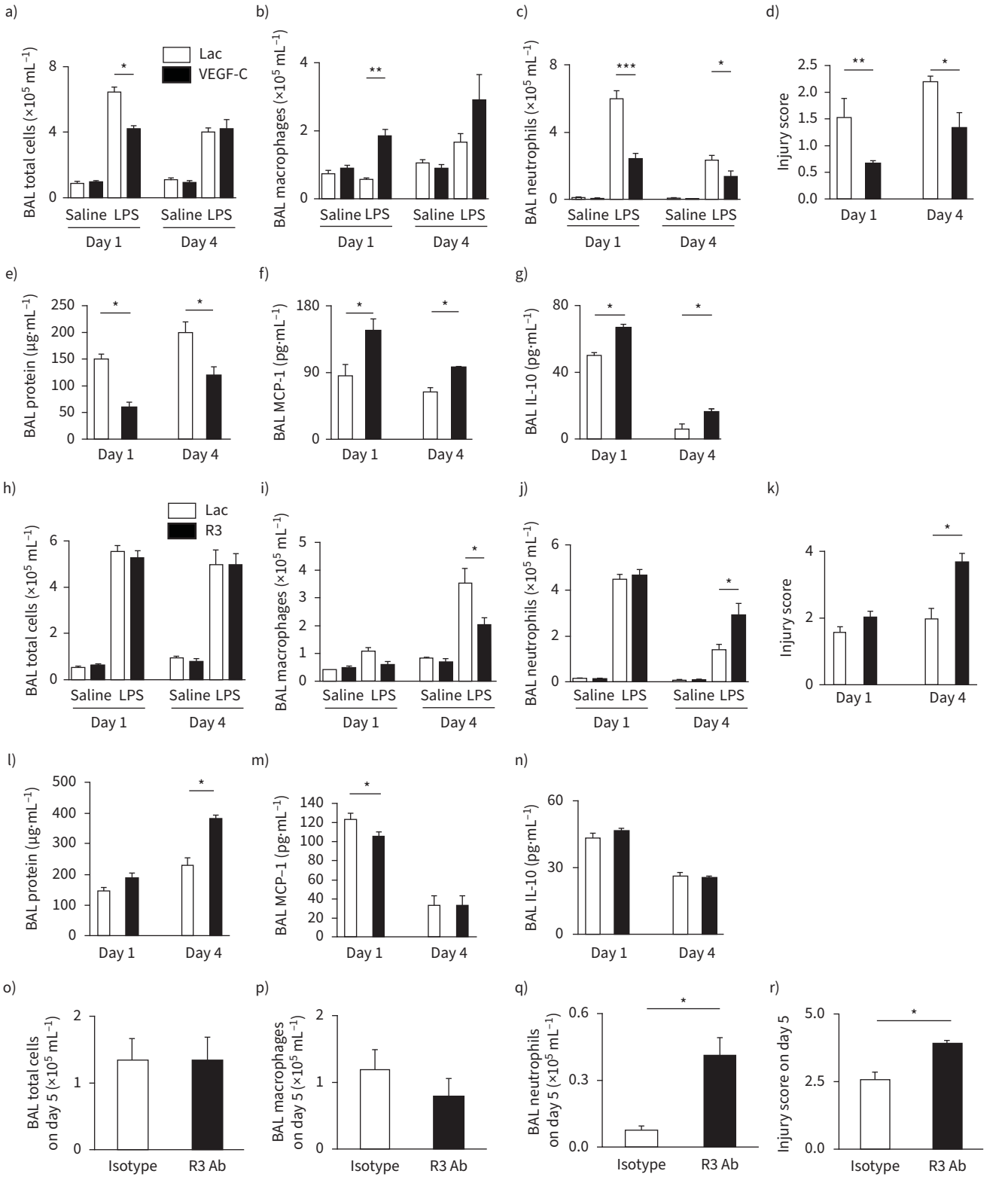

FIGURE 2 Effects of vascular endothelial growth factor (VEGF)-C and soluble VEGF receptor 3 (sVEGFR-3)-Ig in lipopolysaccharide (LPS)-induced lung inflammation/injury models. a–h) Saline as a negative control (n=5 mice per group) or 1.9 mg·kg^{-1} body weight of LPS (n=8 mice per group) was intranasally injected into mice (C57BL/6J) on day 3 after intranasal injection of Ad-VEGF-C (VEGF-C) or Ad-LacZ (Lac) vectors (1.0×10^9 PFU per mouse) and the mice were euthanised the next day or 4 days later. a–c) BAL total cell, macrophage and neutrophil counts. d) Injury score. e) BAL protein concentration. f, g) Concentrations of BAL f) monocyte chemoattractant protein-1 (MCP-1) and g) interleukin-10 (IL-10) determined *via* ELISA. h–n) Saline as a negative control (n=5 mice per group) or 1.9 mg·kg^{-1} body weight of LPS (n=10 mice per group) was intranasally injected

into mice (C57BL/6J) on day 3 after intranasal injection of Ad-sVEGFR-3-Ig (R3) or Ad-LacZ (Lac) vectors (1.0×10^9 PFU per mouse) and the mice were euthanised the next day or 4 days later. h–j) BAL total cell, macrophage and neutrophil counts. k) Injury score. l) BAL protein concentration. m, n) Concentration of BAL m) MCP-1 and n) IL-10 determined *via* ELISA. o–r) Anti-VEGFR-3 blocking antibody (R3 Ab) or isotype control (n=8 mice per group) was intranasally injected into mice (C57BL/6J) on day 3 after intranasal injection of 1.9 mg·kg^{-1} body weight of LPS and the mice were euthanised 2 days later. o–q) BAL total cell, macrophage and neutrophil counts. r) Injury score. Data are presented as mean±SEM. Differences between multiple groups were assessed *via* one-way ANOVA and individual comparisons were analysed using Tukey's test. Differences between two groups were analysed using the t-test. *: p<0.05; **: p<0.01; ***: p<0.001.

anti-VEGFR-3 antibodies than in mice that received isotype control antibodies (figure 2o–r and supplementary figure S1e–f). Hence, we focused on VEGFR-3 expression in macrophages during LPS-induced lung injury.

VEGFR-3$^+$ monocyte lineage cells are involved in recovery from LPS-induced lung injury

We used macrophage Fas-induced apoptosis (Mafia) transgenic mice as a reporter system because in these mice, Green Fluorescent Protein (GFP) is expressed in monocyte colony-stimulating factor (M-CSF) receptor (M-CSFR)-positive cells (supplementary figure S3a) [35]. In fluorescence-activated cell sorting (FACS) analysis, VEGFR-3$^+$M-CSFR$^+$ cells were detected on day 4 in the LPS model (supplementary figure S3b). We sorted two types of M-CSFR$^+$ cells (VEGFR-3$^+$ and VEGFR-3$^-$), in addition to GFP$^-$Ly6G$^+$ neutrophils (supplementary figure S3c). We found that *Flt4* (the VEGFR-3 gene) mRNA levels were significantly higher in VEGFR-3$^+$ cells, thereby validating the results of FACS analyses using anti-VEGFR-3 antibodies (figures S3c–d).

Furthermore, we assessed the kinetics of BAL VEGFR-3$^+$M-CSFR$^+$ cell counts during lung injury using LPS. The number of VEGFR-3$^+$M-CSFR$^+$ cells was considerably increased on days 4 and 5 (figure 3a). We then evaluated mice with a LysM-specific deletion of VEGFR-3 (knockout (KO)), wherein *Flt4* was selectively deleted in myeloid cells, and analysed them in LPS-induced lung injury (supplementary figure S3e). In Kaplan–Meier survival analysis, gene-deleted mice had a shorter survival than control littermates after injection of LPS at 3.8 mg·kg^{-1} body weight (figure 3b). The decline in body weight showed a significant difference between the two groups on days 5 and 6 (figure 3c). In the kinetics of BAL cell counts after LPS injection, neutrophil counts were significantly increased in KO mice on day 5 (figure 3d–f). The injury score and BAL protein concentrations were significantly increased in gene-deleted mice on day 5 (figure 3g–i), although the concentrations of the mediators, including CXCL1, CXCL2, MCP-1, TNF-α, IL-1β, IL-6, IL-17A and IL-10, did not show significant differences throughout the course of the experiments (supplementary figure S4a–h). These results indicated that VEGFR-3$^+$ monocyte lineage cells contributed to the alleviation of LPS-induced lung injury.

VEGF-C/VEGFR-3 signalling facilitates efferocytosis of apoptotic neutrophils via alveolar macrophages

To examine whether VEGF-C/VEGFR-3 signalling was involved in phagocytosis in apoptotic neutrophils, we first identified which subsets of monocyte lineage cells were involved in efferocytosis in a mouse model using intranasal injection of extrinsic UV-irradiated PKH26-labelled apoptotic neutrophils during the recovery phase of LPS-induced lung injury. Over 90% of the apoptotic neutrophils were digested by CD11c$^+$CD11b$^-$F4/80$^+$I-A$^-$ alveolar macrophages (figure 4a and supplementary figure S5a). Cytochalasin D, an actin polymerisation inhibitor, markedly decreased the percentage of PKH26$^+$ cells in M-CSFR$^+$CD11c$^+$CD11b$^-$F4/80$^+$I-A$^-$ alveolar macrophages (supplementary figure S5c). These results indicate that PKH26$^+$ alveolar macrophages represent the digestion of neutrophils by macrophages and not their doublets. We then explored the kinetics of VEGFR-3$^+$ alveolar macrophage counts during LPS-induced lung injury. Because they were consistently increased on day 5 after LPS injection (figure 4b and supplementary figure S5b), we examined the role of VEGF-C/VEGFR-3 signalling in alveolar macrophages. The proportion of alveolar macrophages that phagocytosed extrinsic neutrophils was significantly lower in mice with a LysM-specific VEGFR-3 deletion than in their littermates on day 5 (figure 4c). The results indicated that VEGF-C/VEGFR-3 signalling was at least partially involved in the efferocytosis of apoptotic neutrophils by alveolar macrophages.

Furthermore, we demonstrated that expression of VEGFR-3 in alveolar macrophages of mice that received Ad-VEGF-C vector on day 1 after LPS injection was significantly higher than in mice that received Ad-LacZ vector (figure 4d). On the other hand, *Vegfc* gene expression in BAL cell pellets was significantly less on day 4 after LPS injection in mice that received Ad-sVEGFR-3 vector than in mice that received Ad-LacZ vector, indicating that VEGF-C/VEGFR-3 signalling could function as a positive feedback loop (figure 4e).

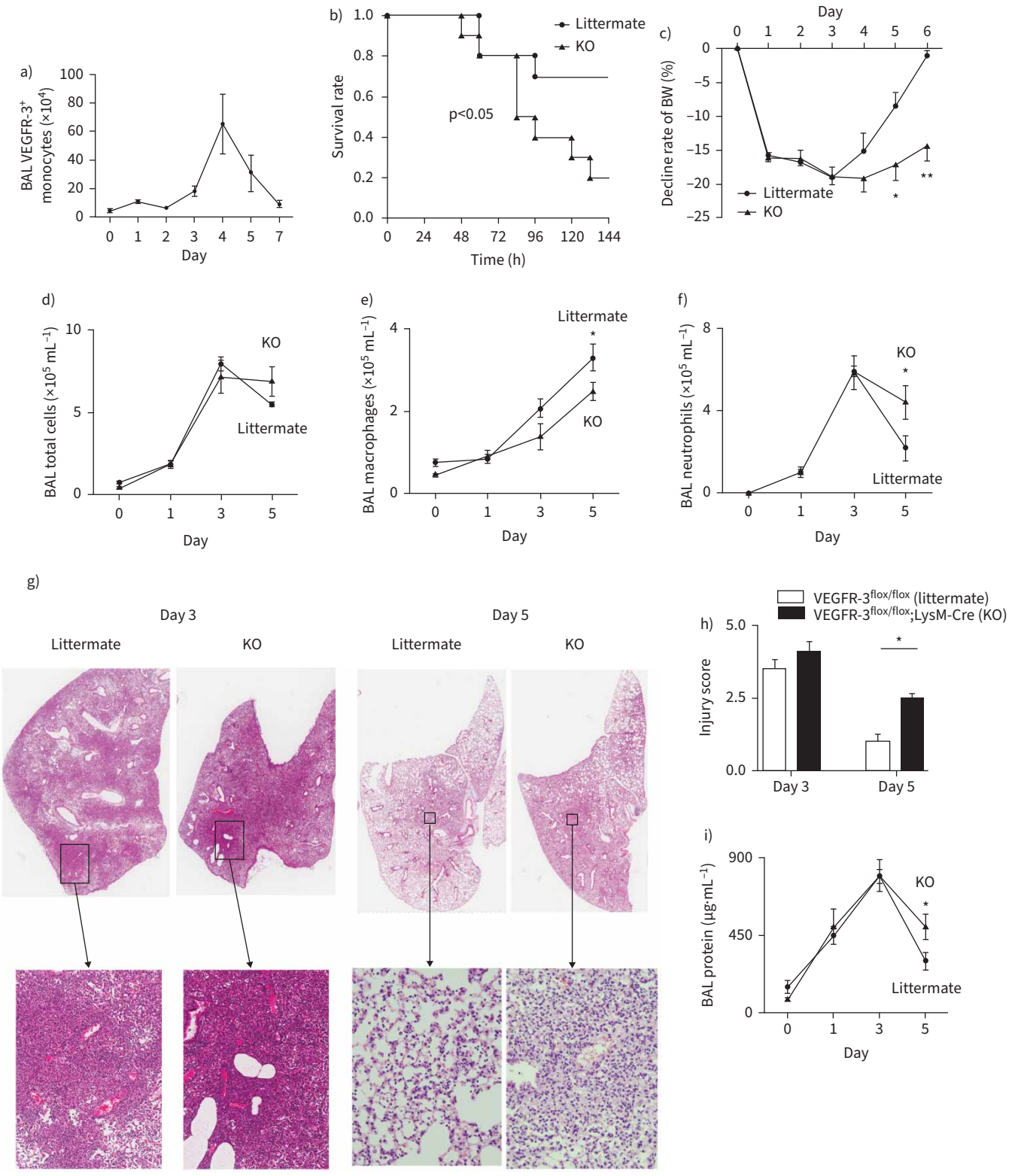

FIGURE 3 Role of vascular endothelial growth factor (VEGF) receptor 3 (VEGFR-3)-positive lineage cells in lipopolysaccharide (LPS)-induced lung injury. a) Cell count kinetics of VEGFR-3^{+} monocyte lineage cells. Mafia mice (n=5 mice per treatment group) were intranasally injected with 1.9 mg·kg^{-1} body weight of LPS, and bronchoalveolar lavage (BAL) VEGFR-3^{+} monocyte lineage cell counts were determined after 1, 2, 3, 4, 5 and 7 days upon cell counting, cell differentiation with May–Giemsa staining and flow cytometry. b) Kaplan–Meier analysis estimates for survival between VEGFR-3$^{flox/flox}$;LysM-Cre mice (knockout (KO)) and VEGFR-3$^{flox/flox}$ mice as control (littermates) after intranasal injection of 3.8 mg·kg^{-1} body weight of LPS (n=11 mice per group). c) Comparison of decline in rates of body weight (BW) from baseline between KO and littermates.

d–f) Kinetics of BAL total cell, macrophage and neutrophil counts. KO and littermates were injected with 3.8 mg·kg^{-1} body weight of LPS and euthanised 1, 3 and 5 days later and before LPS injection on day 0 (n=5 mice in KO and littermates on day 0, n=10 mice in KO and in littermates on days 1, 3 and 5). g) Representative haematoxylin/eosin staining of lung tissue in VEGFR-3$^{flox/flox}$;LysM-Cre mice (KO) and VEGFR-3$^{flox/flox}$ mice as control (littermates) on days 3 and 5 after intranasal injection of 3.8 mg·kg^{-1} body weight of LPS. On day 5, the exudation of alveolar space is remarkably resolved in the littermates, but still remains in an extensive area in KO mice. h, i) During the course of LPS-induced lung injury, h) injury score (on days 3 and 5) and i) BAL protein concentration (on days 0, 1, 3 and 5) were compared between the two groups. Data are presented as mean±SEM. *: p<0.05; **: p<0.01 by log-rank test or t-test.

VEGF-C/VEGFR-3 signalling facilitates efferocytosis via increased CD51 expression

We performed an *in vitro* phagocytosis chamber slide assay using all the cells from BAL fluid collected from Mafia mice at day 4 post-LPS administration. The proportion of M-CSFR$^+$ monocyte lineage cells exhibiting digestion of pHrodo-labelled neutrophils decreased significantly upon treatment with anti-VEGFR-3 antibodies (figure 5a and b). Conversely, we explored whether VEGF-C could enhance efferocytosis in a phagocytic chamber slide assay using alveolar cells obtained by BAL from Mafia mice on day 0. Phagocytosis of neutrophils increased significantly after treatment with recombinant VEGF-C (rVEGF-C), but not after treatment with rVEGF-D or with rVEGF-C combined with anti-VEGFR-3 antibodies (figure 5c). Furthermore, we investigated the molecular mechanisms of efferocytosis stimulation by VEGFR-3 signalling. In the assay involving alveolar macrophages from Mafia mice incubated with rVEGF-C with/without anti-VEGFR-3 blocking antibody, among the phagocytosis-related genes analysed, rVEGF-C treatment caused a significant increase in expression of integrin α_v (*Itgav*) mRNA. Furthermore,

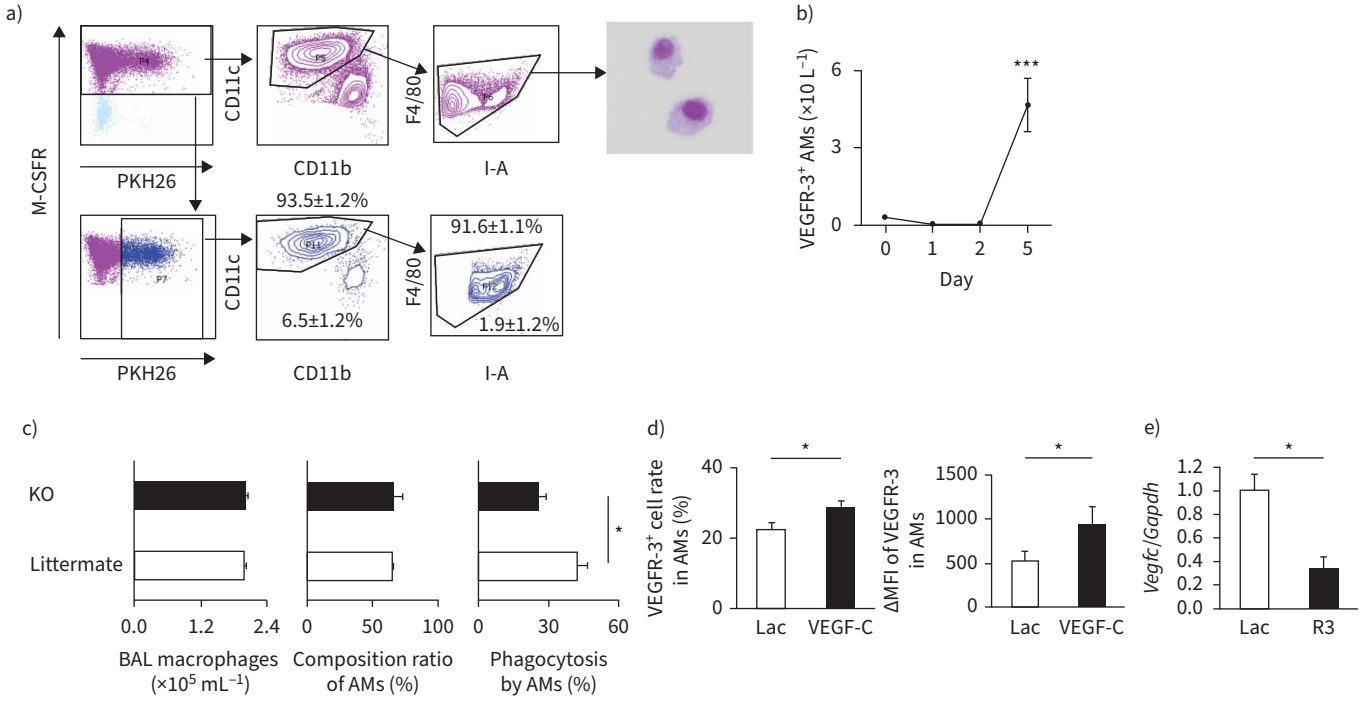

FIGURE 4 Accelerated effects of vascular endothelial growth factor (VEGF)-C/VEGF receptor 3 (VEGFR-3) signalling on efferocytosis of apoptotic neutrophils in alveolar macrophages (AMs). a) Cells obtained from bronchoalveolar lavage (BAL) were used for analyses, and doublets and debris were excluded. Representative plots illustrating the gating strategy to identify the major cells that uptake PKH26-labelled extrinsic apoptotic neutrophils (Mafia mice, n=3). The image represents CD11c$^+$CD11b$^{-\sim moderate}$F4/80$^+$I-A$^-$ cells that are confirmed to be alveolar macrophages. b) Kinetics of VEGFR-3$^+$ alveolar macrophage counts in BAL fluid during the course of lung injury induced by 1.9 mg·kg^{-1} body weight of lipopolysaccharide (LPS) (n=5 per group). c) Phagocytosis rates of alveolar macrophages against 3.0×10^6 apoptotic neutrophils in VEGFR-3$^{flox/flox}$; LysM-Cre (knockout (KO)) mice and littermates on day 5 after 1.9 mg·kg^{-1} body weight of LPS injection (n=5 mice per group). d) Positive rates and change in mean fluorescence intensity (ΔMFI) of VEGFR-3 expression on alveolar macrophages in mice between Ad-VEGF-C (VEGF-C) and Ad-LacZ (Lac) vector on day 1 after intranasal injection of 1.9 mg·kg^{-1} body weight of LPS (n=5 mice per group). e) *Vegfc* mRNA expression was measured in BAL total cell pellets collected on day 1 after LPS injection in mice between Ad-sVEGFR-3-Ig (R3) and Ad-LacZ (Lac) vector. Data are presented as mean±SEM. *: p<0.05 by t-test. M-CSFR: monocyte colony-stimulating factor receptor.

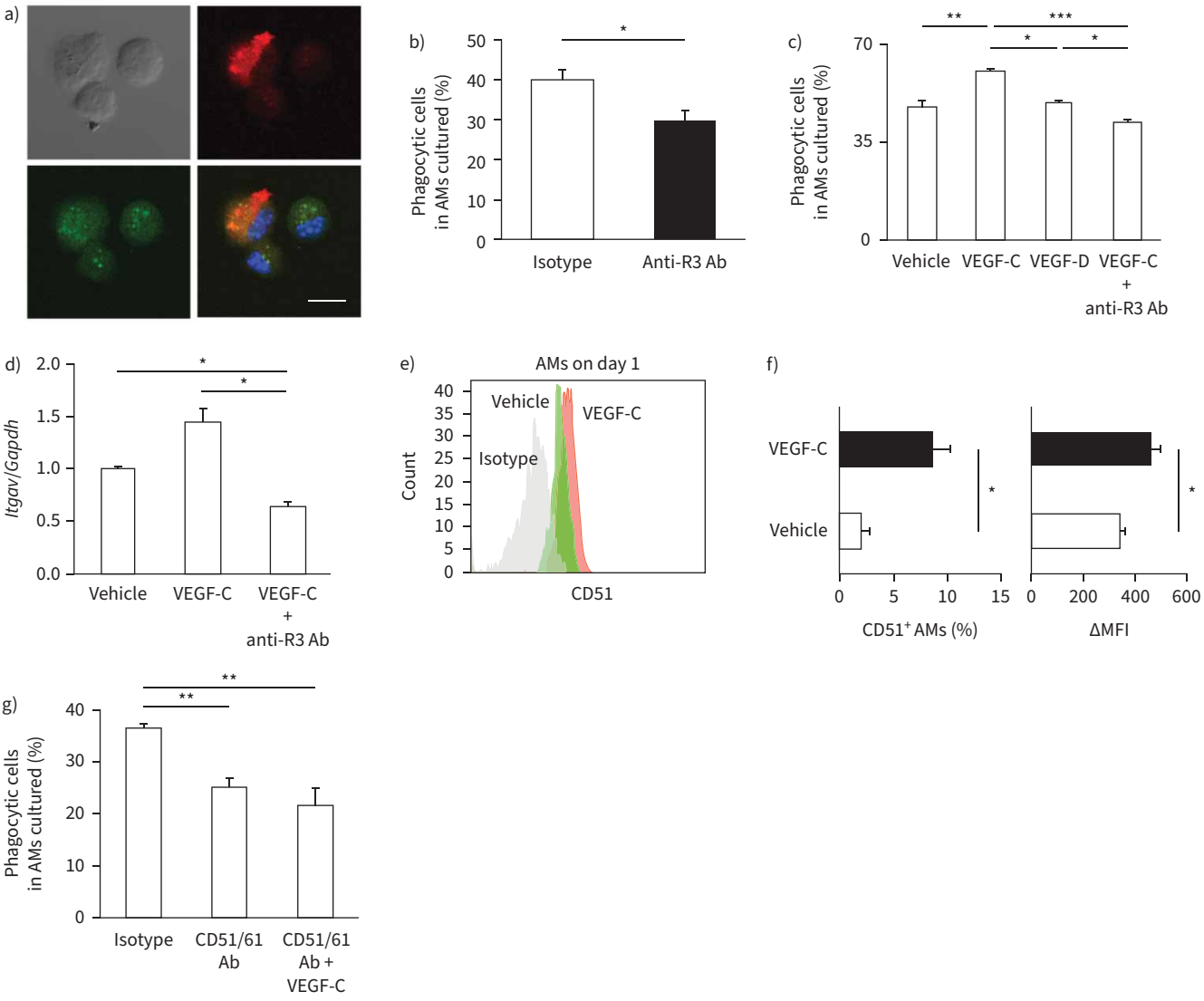

FIGURE 5 Involvement of CD51 on efferocytosis *via* vascular endothelial growth factor (VEGF)-C/VEGF receptor 3 (VEGFR-3) signalling. a) Representative immunofluorescence images of enhanced Green Fluorescence Protein-positive macrophages obtained from bronchoalveolar lavage (BAL) on day 4 (green) after intranasal injection of lipopolysaccharide (LPS) at 0.38 mg·kg^{-1} body weight and pHrodo-labelled digestion of neutrophils (red) in phagocytosis chamber slide assays. Nuclei were labelled with 4′,6-diamidino-2-phenylindole (blue). Scale bar: 10 µm. b) Phagocytosis index of alveolar macrophages (AMs) with anti-VEGFR-3 antibody (anti-R3 Ab) and isotype control treatment (n=5 mice per group). c) The effects of recombinant VEGF-C, VEGF-D and anti-VEGFR-3 blocking antibodies (anti-R3 Ab) were estimated in phagocytosis chamber slide assays using macrophages obtained from BAL on day 0 (n=6 samples per group). d) Gene expression of *Itgav* on alveolar macrophages and their effect on VEGF-C/VEGFR-3 signalling. Alveolar macrophages were harvested by BAL on day 0. After incubation in 12-well plates for 2 h, alveolar macrophages were treated with VEGF-C recombinant protein with/without VEGFR-3 blocking antibody (anti-R3 Ab). After 1 h of incubation, macrophages were harvested. Relative mRNA levels of *Itgav* in the three groups were determined *via* quantitative real-time reverse transcription PCR. e) Fluorescence-activated cell sorting histogram displaying comparable expression of CD51 on alveolar macrophages in mice between recombinant VEGF-C and vehicle control on day 1 after intranasal injection of 0.38 mg·kg^{-1} body weight of LPS. f) Positive rates and change in mean fluorescence intensity (ΔMFI) of CD51 expression (n=5 mice per group). g) Effects of anti-CD51/CD61 blocking antibody (CD51/61 Ab) with/without recombinant VEGF-C were estimated in phagocytosis chamber slide assays using macrophages obtained from BAL on day 0 (n=6 samples per group). Data are presented as mean±SEM. *: p<0.05; **: p<0.01; ***: p<0.001 by t-test or Tukey's *post hoc* test when one-way ANOVA tests were p<0.05.

the anti-VEGFR-3 antibodies inhibited *Itgav* expression (figure 5d and supplementary figure S5b-g). Subsequently, we found that CD51 expression in alveolar macrophages was significantly increased on day 1 in mice that received rVEGF-C (figure 5e and f). In the chamber slide assay, the alveolar macrophage phagocytic index was significantly decreased relative to control after treatment with anti-CD51/CD61

blocking antibody. Furthermore, addition of rVEGF-C did not improve the decline of phagocytic indices after treatment with anti-CD51/CD61 antibody (figure 5g). These results indicate that CD51 signals are involved in the promotion of efferocytosis *via* VEGF-C/VEGFR-3 signalling.

VEGFR-3 expression and its effects of human monocyte-derived macrophages incubated with ARDS BAL fluid

VEGFR-3 was expressed in ∼30% of M-CSF-stimulated human monocyte-derived macrophages (hMDMs) (supplementary figure S6a and b). We incubated the hMDMs with BAL fluid obtained from healthy volunteers and from patients with ARDS and COP for 2 h, and then estimated VEGFR-3 expression in the macrophages. VEGFR-3 expression was significantly decreased in hMDMs incubated in BAL fluid of ARDS patients compared with BAL fluid from the other groups (figure 6a and b). Since the incubation period was short, we presumed that post-translational modification of VEGFR-3 is involved in hMDMs. We found that sVEGFR-3 levels in ARDS BAL fluid increased significantly after incubation with hMDMs compared with that without hMDMs (figure 6c). Irrespective of the presence or absence of hMDMs, no difference in sVEGFR-3 was observed between BAL fluid from COP patients and volunteers.

Finally, we determined IL-10 expression after excess rVEGF-C treatment and monitored efferocytosis capacity in hMDMs incubated with BAL fluid from ARDS and COP patients. IL-10 levels were significantly higher in COP BAL fluid co-incubated with hMDMs than in ARDS BAL fluid, although there was no difference in VEGF-C and IL-10 levels in BAL fluid from ARDS and COP patients (figure 6d and supplementary figure S6d and e). Moreover, IL-10 levels in BAL fluid from COP patients were significantly lower after incubation with hMDMs and anti-VEGFR-3 antibody than that after incubation with hMDM and isotype control antibodies. Conversely, there was no significant difference in IL-10 levels after co-incubating BAL fluid from ARDS patients with hMDMs and anti-VEGFR-3 antibodies or control antibodies (figure 6d). In a phagocytosis chamber slide assay, the proportion of hMDMs exhibiting intracellular pHrodo-labelled murine neutrophils decreased significantly after incubation with BAL fluid from ARDS patients compared with after incubation with BAL fluid from COP patients or healthy volunteers (figure 6e). The phagocytic ratio of hMDMs that were co-incubated with COP BAL fluid and anti-VEGFR-3 antibody was significantly lower than that of hMDMs co-incubated with COP BAL fluid and isotype control. However, the phagocytic ratio of hMDMs did not change significantly after co-incubation with ARDS BAL fluid and anti-VEGFR-3 antibody or isotype control (figure 6f). The *in vitro* experiments in alveolar macrophages from VEGFR-3$^{flox/flox}$;LysM-Cre mice and littermates (supplementary figure S6f) showed that the relationship between VEGFR-3 signalling in macrophages and COP and ARDS BAL fluid was the same as that observed for hMDMs. Moreover, the phagocytic ratio in hMDMs increased significantly after rVEGF-C treatment and decreased after treatment with VEGFR-3 and/or CD51/CD61 blocking antibodies (figure 6g and h). These results suggest that the decline in IL-10 expression and efferocytosis in hMDMs co-incubated with ARDS BAL fluid was, at least partially, due to an interference in VEGFR-3 signalling.

Discussion

Only a few studies have reported the role of VEGFR-3^{+} macrophages in lung injury. Zhang *et al*. [31] reported that VEGFR-3 signalling in macrophages contributes to prolonged survival and decreased degree of lung injury in a sepsis model induced by a super-high dose of LPS *via* suppression of Toll-like receptor 4/NF-κB signalling and pro-inflammatory cytokines. In the present study, the overexpression of VEGF-C using Ad-VEGF-C vector alleviated lung injury with increased levels of BAL IL-10 in the early phase. Conversely, inhibition of VEGF-C/VEGFR-3 signalling using Ad-sVEGFR-3-Ig or using mice with a LysM-driven *Vegfr3* gene deletion worsened lung injury only during the later phase. In addition, inhibition of VEGFR-3 signalling *via* anti-VEGFR-3 antibodies after the creation of clinically relevant lung injury delayed the resolution of lung injury. Our results suggest that VEGF-C/VEGFR-3 signalling in macrophages may play multiple roles in the amelioration of acute lung injury, including anti-inflammatory functions in the early phase and restorative functions that are unique to the later phase.

We demonstrated that alveolar macrophages are potential phagocytes of apoptotic neutrophils and that inhibition of VEGF-C/VEGFR-3 signalling decreased alveolar macrophage phagocytic activity towards neutrophil efferocytosis, in both *in vivo* and *ex vivo* experiments. These findings suggest that efferocytosis by alveolar macrophages *via* VEGF-C/VEGFR-3 signalling may indispensably participate in the resolution in the later phase of acute lung injury. Furthermore, both in murine and human studies, we found that CD51 signalling in macrophages is at least partially involved in efferocytosis *via* VEGF-C/VEGFR-3 signalling. CD51 is part of the most important receptor that mediates phagocytosis of apoptotic cells *via* heterodimerisation with β_3 (CD51/CD61) [21–23]. Further investigations should determine the detailed mechanisms by which CD51 signalling is involved in efferocytosis, including cell binding and engulfment [37].

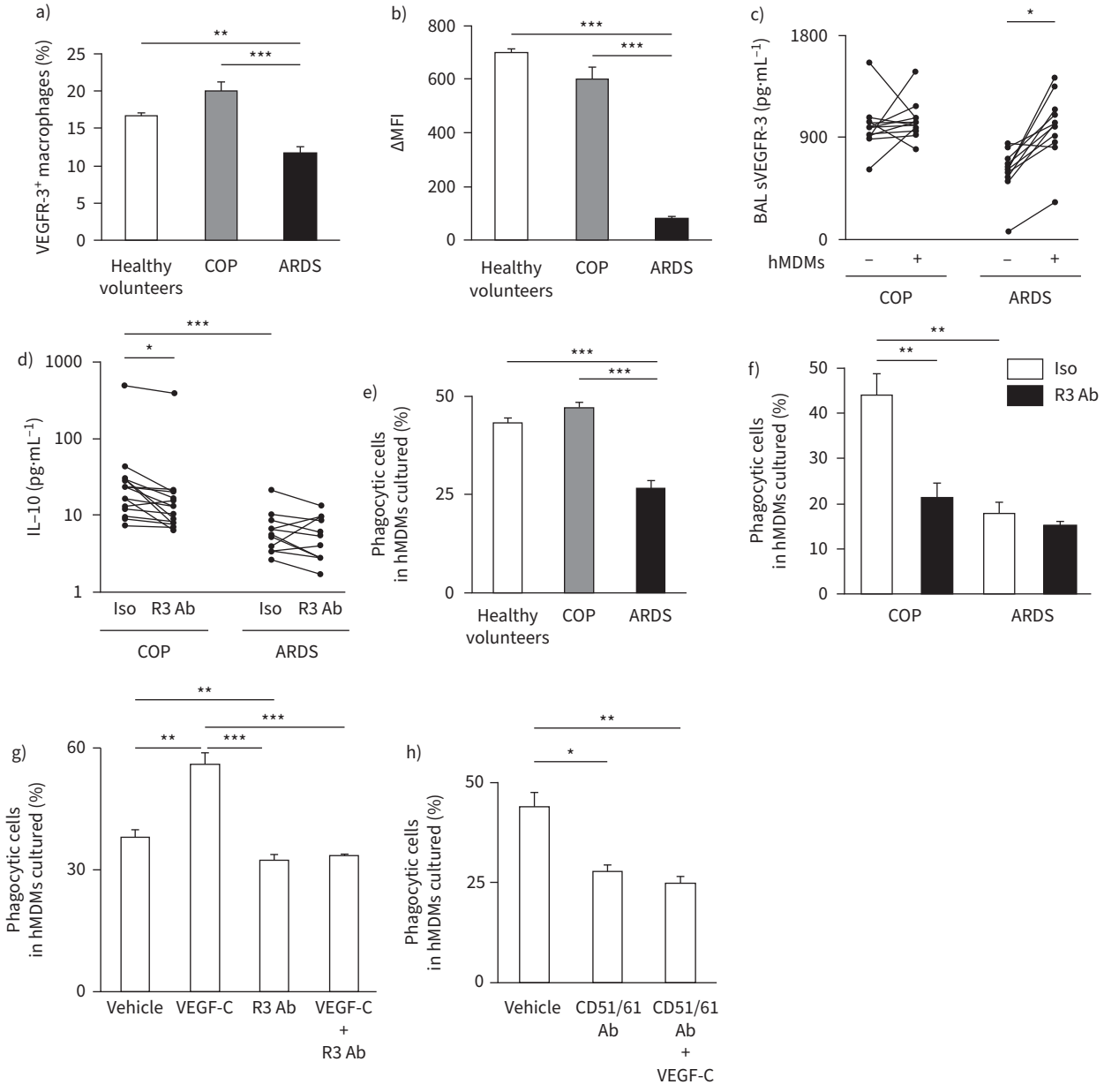

FIGURE 6 Vascular endothelial growth factor receptor 3 (VEGFR-3) expression and its effects in human monocyte-derived macrophages (hMDMs) when incubated with bronchoalveolar lavage (BAL) fluid of patients with acute respiratory distress syndrome (ARDS). a, b) VEGFR-3^{+} rate and change in mean fluorescence intensity (ΔMFI) of hMDMs when incubated with BAL fluid obtained from healthy volunteers (n=18), ARDS patients (n=12) or cryptogenic organising pneumonia (COP) patients (n=14) were estimated by fluorescence-activated cell sorting. c) Individual comparisons of soluble VEGFR-3 (sVEGFR-3) concentration determined *via* ELISA in BAL fluid obtained from patients with COP (n=14) and ARDS (n=12) that were co-incubated with and without hMDMs (COP 984.5±65.9 *versus* 1043.1±50.4 pg·mL^{-1}; ARDS 592.4±61.2 *versus* 991.5±87.1 pg·mL^{-1}). d) Individual comparisons of interleukin-10 (IL-10) concentrations determined *via* ELISA in BAL fluid obtained from patients with COP (n=10) and ARDS (n=10) that were co-incubated with hMDMs, and anti-VEGFR-3 antibody (R3 Ab) or isotype controls (Iso) under treatment with 100 ng·mL^{-1} VEGF-C (COP 52.5±30.3 *versus* 38.0±23.8 pg·mL^{-1}; ARDS 7.0±1.3 *versus* 6.0±0.9 pg·mL^{-1}). e) Phagocytosis rate of hMDMs against mural apoptotic neutrophils when incubated with BAL fluid obtained from healthy volunteers (n=18) and patients with ARDS (n=12) and COP (n=14) were assessed in a chamber slide assay using pHrodo-labelled digestion of neutrophils obtained from murine spleen. f) Phagocytosis rate of hMDMs when co-incubated with BAL fluid of patients with COP (n=14) or ARDS (n=12) and anti-VEGFR-3 antibody (R3 Ab) or isotype control (Iso). g) Phagocytosis rate of hMDMs treated with recombinant VEGF-C and/or anti-VEGFR-3 antibody (R3 Ab) was assessed in a phagocytosis chamber slide assay using pHrodo-labelled digestion of neutrophils obtained from murine spleen (n=6 samples per groups). h) Phagocytosis rate of hMDMs treated with anti-CD51/CD61 antibody (CD51/61 Ab) and/or recombinant VEGF-C (n=6 samples per groups) was assessed in a phagocytosis chamber slide assay using pHrodo-labelled digestion of neutrophils obtained from murine spleen. Data are presented as mean±SEM. *: p<0.05; **: p<0.01; ***: p<0.001 by t-test and paired sample t-test or Tukey's *post hoc* test when one-way ANOVA tests were p<0.05.

In hMDMs, we observed a decrease in VEGFR-3 and IL-10 expression and efferocytosis capacity when hMDMs were co-incubated with BAL fluid from ARDS patients. Consistently, recent papers reported impaired efferocytosis in MDMs and alveolar macrophages from ARDS patients [38, 39]. However, we could not compare the functional differences in VEGFR-3 signalling on macrophages between ARDS patients and patients with neutrophilic lung inflammation without ARDS. In addition, it should be noted that Misharin *et al*. [40] reported that tissue-resident alveolar macrophages exhibit different characteristics from monocyte-derived alveolar macrophages [40]. In our study, we could not determine the effect of VEGFR-3 signalling in alveolar macrophages from COP and ARDS patients. Consequently, we could not conclude if our findings on the role of VEGFR-3 signalling in hMDMs are also relevant to alveolar macrophages from COP and ARDS patients. On the other hand, we observed a marked increase in sVEGFR-3 levels in ARDS BAL fluid incubated with hMDMs. This suggests that the initial decrease in VEGFR-3 levels observed after co-incubating hMDMs with ARDS BAL fluid was due to the cleavage of its extracellular domain. Thus, we hypothesised that cleavage of VEGFR-3 in macrophages located in the alveolar space impairs resolution in ARDS by decreasing IL-10 expression and efferocytosis capacity.

In conclusion, our study indicates that VEGF-C/VEGFR-3 signalling in macrophages ameliorates acute lung injury *via* multiple mechanisms, such as limiting inflammation in the acute phase and efferocytosis in the later phase. Furthermore, we suggest that this protective function of macrophages is potentially impaired in humans during ARDS due to the decreased expression of VEGFR-3 on macrophages.

Author contributions: M. Yamashita designed and performed the experiments, analysed the data, and wrote the manuscript. M. Niisato, Y. Kawasaki, S. Karaman and M.R. Robciuc assisted with various experiments, some done in the laboratory of K. Alitalo. Y. Shibata, T. Masuda and T. Sugai assisted with the histopathological analysis. Y. Ishida assisted with the flow cytometry experiments. R. Nishio assisted with the preparation of adenovirus vectors. M. Ono and R.M. Tuder provided crucial advice.

Conflict of interest: None declared.

Support statement: M. Yamashita acknowledges partial support from JSPS KAKENHI (JP16K08940 and JP19K07894). Funding information for this article has been deposited with the Crossref Funder Registry.

References

1 Andrews T, Sullivan KE. Infections in patients with inherited defects in phagocytic function. *Clin Microbiol Rev* 2003; 16: 597–621.
2 Kurahashi K, Sawa T, Ota M, *et al.* Depletion of phagocytes in the reticuloendothelial system causes increased inflammation and mortality in rabbits with *Pseudomonas aeruginosa* pneumonia. *Am J Physiol Lung Cell Mol Physiol* 2009; 296: L198–L209.
3 Moore KW, Vieira P, Fiorentino DF, *et al.* Homology of cytokine synthesis inhibitory factor (IL-10) to the Epstein-Barr virus gene BCRFI. *Science* 1990; 248: 1230–1234.
4 Fiorentino DF, Bond MW, Mosmann TR. Two types of mouse T helper cell. IV. Th2 clones secrete a factor that inhibits cytokine production by Th1 clones. *J Exp Med* 1989; 170: 2081–2095.
5 Savill JS, Wyllie AH, Henson JE, *et al.* Macrophage phagocytosis of aging neutrophils in inflammation. Programmed cell death in the neutrophil leads to its recognition by macrophages. *J Clin Invest* 1989; 83: 865–875.
6 Cox G, Crossley J, Xing Z. Macrophage engulfment of apoptotic neutrophils contributes to the resolution of acute pulmonary inflammation *in vivo*. *Am J Respir Cell Mol Biol* 1995; 12: 232–237.
7 Morimoto K, Amano H, Sonoda F, *et al.* Alveolar macrophages that phagocytose apoptotic neutrophils produce hepatocyte growth factor during bacterial pneumonia in mice. *Am J Respir Cell Mol Biol* 2001; 24: 608–615.
8 Weissmann G, Smolen JE, Korchak HM. Release of inflammatory mediators from stimulate neutrophils. *N Engl J Med* 1980; 303: 27–34.
9 Travis WD, Colby TV, Koss MN, *et al.* Non-neoplastic Disorders of the Lower Respiratory Tract (Atlas of Nontumor Pathology). Washington, American Registry of Pathology and Armed Forces Institute of Pathology, 2002.
10 Li J, Zhan QY, Wang C. Survey of prolonged mechanical ventilation in intensive care units in mainland China. *Respir Care* 2016; 61: 1224–1231.
11 Kong MY, Li Y, Oster R, *et al.* Early elevation of matrix metalloproteinase-8 and -9 in pediatric ARDS is associated with an increased risk of prolonged mechanical ventilation. *PLoS One* 2011; 6: e22596.
12 Braune S, Schönhofer B. Prolonged weaning in patients with ARDS. *Dtsch Med Wochenschr* 2017; 142: 102–109.
13 Yoshimura T, Yuhki N, Moore SK, *et al.* Human monocyte chemoattractant protein-1 (MCP-1). Full-length cDNA cloning, expression in mitogen-stimulated blood mononuclear leukocytes, and sequence similarity to mouse competence gene JE. *FEBS Lett* 1989; 244: 487–493.

14 Chen F, Liu Z, Wu W, *et al.* An essential role for TH2-type responses in limiting acute tissue damage during experimental helminth infection. *Nat Med* 2012; 18: 260–266.
15 Liu YW, Chen CC, Tseng HP, *et al.* Lipopolysaccharide-induced transcriptional activation of interleukin-10 is mediated by MAPK- and NF-kappaB-induced CCAAT/enhancer-binding protein delta in mouse macrophages. *Cell Signal* 2006; 18: 1492–1500.
16 Hos D, Bucher F, Regenfuss B, *et al.* IL-10 indirectly regulates corneal lymphangiogenesis and resolution of inflammation via macrophages. *Am J Pathol* 2016; 186: 159–171.
17 Grabiec AM, Hussell T. The role of airway macrophages in apoptotic cell clearance following acute and chronic lung inflammation. *Semin Immunopathol* 2016; 38: 409–423.
18 Freeman GJ, Casasnovas JM, Umetsu DT, *et al.* TIM genes: a family of cell surface phosphatidylserine receptors that regulate innate and adaptive immunity. *Immunol Rev* 2010; 235: 172–189.
19 Ramachandran P, Pellicoro A, Vernon MA, *et al.* Differential Ly-6C expression identifies the recruited macrophage phenotype, which orchestrates the expression of murine liver fibrosis. *Proc Natl Acad Sci USA* 2012; 109: E3186–E3195.
20 Savill J, Hogg N, Ren Y, *et al.* Thrombospondin cooperates with CD36 and the vitronectin receptor in macrophage recognition of neutrophils undergoing apoptosis. *J Clin Invest* 1992; 90: 1513–1522.
21 Stem M, Savill J, Haslett C. Human monocyte-derived macrophage phagocytosis of senescent eosinophils undergoing apoptosis. Mediation by $\alpha_v\beta_3$/CD36/thrombospondin recognition mechanism and lack of phlogistic response. *Am J Pathol* 1996; 149: 911–921.
22 Hughes J, Liu Y, Van Damme J, *et al.* Human glomerular mesangial cell phagocytosis of apoptotic neutrophils: mediation by a novel CD36-independent vitronectin receptor/thrombospondin recognition mechanism that is uncoupled from chemokine secretion. *J Immunol* 1997; 158: 4389–4397.
23 Welser-Alves JV, Boroujerdi A, Tigges U, *et al.* Microglia use multiple mechanisms to mediate interactions with vitronectin; non-essential roles for the highly expressed αvβ3 and αvβ5 integrins. *J Neuroinflammation* 2011; 8: 157.
24 Alitalo, K. The lymphatic vasculature in disease. *Nat Med* 2011; 17: 1371–1380.
25 Yamashita M, Iwama N, Date F, *et al.* Macrophages participate in lymphangiogenesis in idiopathic diffuse alveolar damage through CCL19-CCR7 signal. *Hum Pathol* 2009; 40: 1553–1563.
26 Jeltsch M, Kaipainen A, Joukov V, *et al.* Hyperplasia of lymphatic vessels in VEGF-C transgenic mice. *Science* 1997; 276: 1423–1425.
27 Karkkainen MJ, Haiko P, Sainio K, *et al.* Vascular endothelial growth factor C is required for sprouting of the first lymphatic vessels from embryonic veins. *Nat Immunol* 2004; 5: 74–80.
28 Veikkola T, Jussila L, Makinen T, *et al.* Signalling via vascular endothelial growth factor receptor-3 is sufficient for lymphangiogenesis in transgenic mice. *EMBO J* 2001; 20: 1223–1231.
29 Nykänen AI, Sandelin H, Krebs R, *et al.* Targeting lymphatic vessel activation and CCL21 production by vascular endothelial growth factor receptor-3 inhibition has novel immunomodulatory and antiarteriosclerotic effects in cardiac allografts. *Circulation* 2010; 121: 1413–1422.
30 Maruyama K, Ii M, Cursiefen C, *et al.* Inflammation-induced lymphangiogenesis in the cornea arises from CD11b-positive macrophages. *J Clin Invest* 2005; 115: 2363–2372.
31 Zhang Y, Lu Y, Ma L, *et al.* Activation of vascular endothelial growth factor receptor-3 in macrophages restrains TLR4-NF-κB signaling and protects against endotoxin shock. *Immunity* 2014; 40: 501–514.
32 Kerjaschki D, Huttary N, Raab I, *et al.* Lymphatic endothelial progenitor cells contribute to *de novo* lymphangiogenesis in human renal transplants. *Nat Med* 2006; 12: 230–234.
33 Burnett SH, Kershen EJ, Zhang J, *et al.* Conditional macrophage ablation in transgenic mice expressing a Fas-based suicide gene. *J Leukoc Biol*. 2004; 75: 612–623.
34 Krebs R, Tikkanen JM, Ropponen JO, *et al.* Critical role of VEGF-C/VEGFR-3 signaling in innate and adaptive immune responses in experimental obliterative bronchiolitis. *Am J Pathol* 2012; 181: 1607–1620.
35 Baluk P, Tammela T, Ator E, *et al.* Pathogenesis of persistent lymphatic vessel hyperplasia in chronic airway inflammation. *J Clin Invest* 2005; 115: 247–257.
36 Katzenstein A-LA. Acute lung injury patterns: diffuse alveolar damage and bronchiolitis obliterans-organizing pneumonia. *In*: Katzenstein A-LA, ed. Katzenstein and Askin's Surgical Pathology of Non-neoplastic Lung Disease. 3rd Edn. Philadelphia, Saunders, 1997; pp. 14–47.
37 Krispin A, Bledi Y, Atallah M, *et al.* Apoptotic cell thrombospondin-1 and heparin-binding domain lead to dendritic-cell phagocytic and tolerizing states. *Blood* 2006; 108: 3580–3589.
38 Grégoire M, Uhel F, Lesouhaitier M, *et al.* Impaired efferocytosis and neutrophil extracellular trap clearance by macrophages in ARDS. *Eur Respir J* 2018; 52: 1702590.
39 Mahida RY, Scott A, Parekh D, *et al.* Acute respiratory distress syndrome is associated with impaired alveolar macrophage efferocytosis. *Eur Respir J* 2021; 58: 2100829.
40 Misharin AV, Morales-Nebreda L, Reyfman PA, *et al.* Monocyte-derived alveolar macrophages drive lung fibrosis and persist in the lung over the life span. *J Exp Med* 2017; 214: 2387–2404.